Int J Thermophys (2012) 33:1876–1886
DOI 10.1007/s10765-012-1264-3

Simultaneous Measurement of Thermal Diffusivity and Optical Absorption Coefficient of Solids Using PTR and PPE: A Comparison

R. Fuente · A. Mendioroz · E. Apiñaniz · A. Salazar

Received: 10 January 2012 / Accepted: 17 July 2012 / Published online: 17 August 2012

Abstract Modulated photothermal radiometry (PTR) and a modulated photopyroelectric (PPE) technique have been widely used to measure the thermal diffusivity of bulk materials. The method is based on illuminating the sample with a plane light beam and measuring the infrared emission with an infrared detector (PTR) or the electric voltage produced by a pyroelectric sensor in contact with the sample (PPE). The amplitude and phase of both photothermal signals are recorded as a function of the modulation frequency and then fitted to the theoretical model. In this work, we compare the ability of modulated PTR and PPE to retrieve simultaneously the thermal diffusivity and the optical absorption coefficient of homogeneous slabs. In order to eliminate the instrumental factor, self-normalization is used, i.e., the ratio of the photothermal signal recorded at the rear and front surfaces. The influence of the multiple reflections of the light beam and the transparency to infrared wavelengths are analyzed. Measurements performed on a wide variety of homogeneous materials, transparent and opaque, good and bad thermal conductors, confirm the validity of the method. The advantages and disadvantages of both techniques are discussed.

Keywords Optical absorption coefficient · Photopyroelectric technique · Photothermal radiometry · Thermal diffusivity

R. Fuente · A. Mendioroz · A. Salazar (✉)
Departamento de Física Aplicada I, Escuela Técnica Superior de Ingeniería, Universidad del País Vasco, Alameda Urquijo s/n, 48013 Bilbao, Spain
e-mail: agustin.salazar@ehu.es

E. Apiñaniz
Departamento de Física Aplicada I, Escuela Universitaria de Ingeniería, Universidad del País Vasco, Nieves Cano 12, 01006 Vitoria-Gasteiz, Spain

1 Introduction

Modulated photothermal radiometry (PTR) consists of illuminating the sample by an intensity modulated light beam and detecting the oscillating component of the temperature rise by means of an infrared detector connected to a lock-in amplifier [1]. In turn, the modulated photopyroelectric (PPE) technique records the electric voltage produced by a pyroelectric sensor in contact with the sample [2,3]. As the temperature rise of the sample depends on its thermal properties, modulated PTR and PPE have been widely used to measure the thermal diffusivity of a large variety of materials [4–6].

Moreover, some photothermal techniques (photoacoustic spectroscopy or the mirage effect) have proven to be very reliable for the purpose of measuring the optical absorption coefficient of gases, liquids, and solids. These techniques compete with success against optical techniques in the extreme cases of weakly or highly absorbing materials [7–9].

In modulated PTR and PPE with plane illumination, the amplitude and phase of the photothermal signal is recorded as a function of the modulation frequency and then fitted to the theoretical model. However, normalization procedures are needed in order to suppress the instrumental factor, i.e., the dependence of the detection electronics on frequency. Among the different normalization procedures, we have selected the self-normalization method (which consists in dividing the PTR signals recorded at the rear and front surfaces [10]) since it provides the highest signal-to-noise ratio and amplitude and phase contrast.

The aim of this work is to compare the ability of modulated PTR and PPE to retrieve simultaneously and accurately the optical absorption coefficient (α) and the thermal diffusivity (D) of homogeneous slabs. First, we have studied the theory of PTR and PPE signal generation, including some additional effects such as the multiple reflection of the exciting light beam at the sample surfaces and the transparency of the sample to IR wavelengths. Then we have performed modulated PTR and PPE measurements on a wide variety of materials: from opaque to transparent and from good to poor thermal conductors. The advantages and drawbacks of both techniques are discussed.

1.1 Theory

In this section we discuss the photothermal signal generation in the case of free standing semitransparent slabs. We consider ideal conditions: (a) absence of heat losses to the surrounding media, (b) absence of internal reflections of the exciting light beam inside the slab, and (c) no light diffusion inside the sample.

1.2 PTR Signal

Let us consider a semitransparent slab of thickness L, illuminated by a light beam of wavelength λ, and intensity I_o modulated at a frequency $f(\omega = 2\pi f)$. The geometry of the problem is shown in Fig. 1. According to the Beer–Lambert law, the light intensity inside the sample in the front and back configurations are given by I_{front}

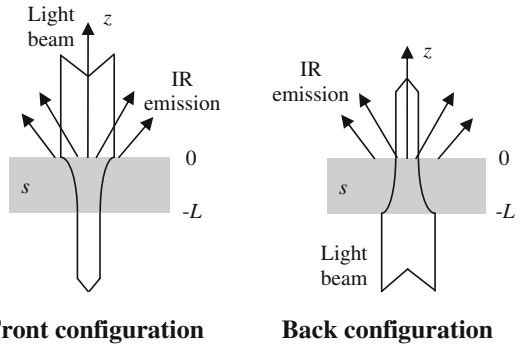

Fig. 1 Scheme of the generation of the PTR signal corresponding to a semitransparent slab illuminated by a modulated light beam

$(z) = I_o\,(1-R)\,e^{\alpha z}$, $I_{back}\,(z) = I_o\,(1-R)\,e^{-\alpha(z+L)}$, where R and α are the optical reflection and absorption coefficients of the slab at the wavelength of the light beam, respectively. By solving the heat diffusion equation with adiabatic boundary conditions, the oscillating component of the temperature is obtained [11]:

$$T_{front}(z) = \frac{I_o\,(1-R)\,\alpha^2}{2Kq\left(q^2-\alpha^2\right)} \left[\frac{\left(e^{-\alpha L}-e^{qL}\right)e^{qz}+\left(e^{-\alpha L}-e^{-qL}\right)e^{-qz}+\frac{q}{\alpha}\left(e^{qL}-e^{-qL}\right)e^{\alpha z}}{e^{qL}-e^{-qL}}\right], \tag{1a}$$

$$T_{back}(z) = \frac{I_o\,(1-R)\,\alpha^2}{2Kq\left(q^2-\alpha^2\right)} \left[\frac{\left(e^{-\alpha L}-e^{qL}\right)e^{-q(z+L)}+\left(e^{-\alpha L}-e^{-qL}\right)e^{q(z+L)}+\frac{q}{\alpha}\left(e^{qL}-e^{-qL}\right)e^{-\alpha(z+L)}}{e^{qL}-e^{-qL}}\right], \tag{1b}$$

where $q = \sqrt{i\omega/D}$ is the thermal wave vector and K is the thermal conductivity of the sample.

If the sample is opaque to IR wavelengths, the PTR signal is proportional to the sample surface temperature oscillation $S_{PTR} \propto T\,(0)$ [12]. Accordingly, the self-normalized PTR signal is given by

$$S_{PTR,n} = \frac{S_{PTR,back}}{S_{PTR,front}} = \frac{T_{back}(0)}{T_{front}(0)} = \frac{\alpha - e^{-\alpha L}\left[\alpha\cosh(qL)+q\sinh(qL)\right]}{\alpha\cosh(qL)-q\sinh(qL)-\alpha e^{-\alpha L}}. \tag{2}$$

As can be seen, the self-normalized temperature depends on $L/\sqrt{D}$ and on αL, but does not depend on K. Therefore both α and D can be retrieved simultaneously.

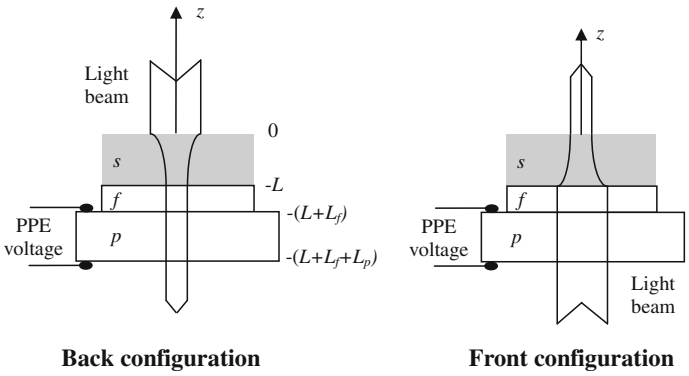

Fig. 2 Scheme of the generation of the PPE signal corresponding to a semitransparent slab illuminated by a modulated light beam

1.3 PPE Signal

Now we consider the same slab as before, but in contact with a pyroelectric plate by means of a thin coupling fluid layer. Both the fluid and the pyroelectric are transparent to the light wavelength. The geometry of the problem is shown in Fig. 2. The PPE signal is proportional to the average temperature of the pyroelectric plate, $S_{\mathrm{PPE}} \propto \langle T_{\mathrm{p}} \rangle = \frac{1}{L_{\mathrm{p}}} \int_{-(L+L_{\mathrm{f}}+L_{\mathrm{p}})}^{-(L+L_{\mathrm{f}})} T_{\mathrm{p}}(z)\mathrm{d}z$ [13]. Subscripts f and p correspond to fluid and pyroelectric sensor, respectively. By solving the heat diffusion equation for each layer, the self-normalized PPE signal is obtained:

$$S_{\mathrm{PPE,n}} = \frac{S_{\mathrm{PPE,back}}}{S_{\mathrm{PPE,front}}} = \frac{\langle T_{\mathrm{p}} \rangle_{\mathrm{back}}}{\langle T_{\mathrm{p}} \rangle_{\mathrm{front}}} = \frac{\alpha - \mathrm{e}^{-\alpha L}\left[\alpha \cosh(qL) + q \sinh(qL)\right]}{\alpha \cosh(qL) - q \sinh(qL) - \alpha \mathrm{e}^{-\alpha L}}. \quad (3)$$

Note that $S_{\mathrm{PPE,n}} = S_{\mathrm{PTR,n}} = S_{\mathrm{n}}$, i.e., both techniques can be applied in the same way to extract information on the thermal and optical properties of semitransparent samples.

1.4 Discussion

Three main cases can be distinguished: (a) If the slab is opaque ($\alpha L \to \infty$) and thermally thick ($qL \to \infty$), Eqs. 2 and 3 reduce to $S_{\mathrm{n}} \approx 2\mathrm{e}^{-qL}$, indicating that both the natural logarithm of the amplitude of the self-normalized PTR and PPE signals, $\ln(|S_{\mathrm{n}}|)$, and their phase, $\Psi(S_{\mathrm{n}})$, are parallel straight lines when plotted against $\sqrt{f}$, with the same slope $m = -L\sqrt{\pi/D}$. This equation provides a well-known method to measure the thermal diffusivity of opaque slabs [14]. (b) If the sample is transparent ($\alpha L \to 0$), Eqs. 2 and 3 reduce to $S_{\mathrm{n}} \approx 1$, so that no information on the thermal and optical properties of the sample can be retrieved. (c) For semitransparent samples, the frequency scan of the self-normalized photothermal signal S_{n} must be fitted to

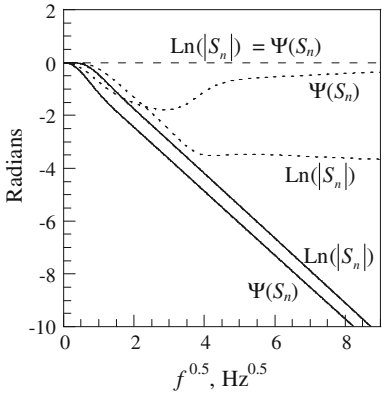

Fig. 3 Calculations of $\ln(|S_n|)$ and $\Psi(S_n)$ as a function of $\sqrt{f}$ for a glass slab 0.5 mm thick ($D = 0.5\ \mathrm{mm}^2 \cdot \mathrm{s}^{-1}$). Three absorption coefficients have been considered: (a) opaque material ($\alpha \to \infty$), *continuous line*; (b) transparent material ($\alpha \to 0$), *dashed line*; and (c) semitransparent material ($\alpha = 8\ \mathrm{mm}^{-1}$), *dotted line*

Eqs. 2 or 3. The three cases are shown in Fig. 3 , where calculations have been performed for a glass slab ($D = 0.5\,\mathrm{mm}^2 \cdot \mathrm{s}^{-1}$) 0.5 mm thick.

Numerical calculations indicate that a sample behaves as transparent when $\alpha L < 0.8$, and as opaque when $\alpha L > 10$. Between these values the sample is semitransparent and therefore both D and α can be retrieved. Even though that range seems very restrictive, it corresponds to optical transmissions ranging from 0.5 to 4×10^{-5}, i.e., five orders of magnitude.

Now we address the issue of whether D and α are degenerate. Let us define g, a residual function, as follows:

$$g(D, \alpha) = \frac{1}{2} \sum_{j=1}^{N} \left| S_{\mathrm{n,theory}}\left(D, \alpha, f_j\right) - S_{\mathrm{n,measured}}(f_j) \right|^2, \tag{4}$$

where $S_{\mathrm{n,measured}}$ is the experimental value of the self-normalized photothermal signal (amplitude or phase) at a frequency f_i and $S_{\mathrm{n,theory}}$ is the theoretical value at that frequency, calculated by means of Eqs. 2 or 3. The sum runs over all N modulation frequencies of the experiment. Now, the determination of D and α is reduced to finding the set of parameters that minimizes g. To visualize this function, we show in Fig. 4 its contour plot for a glass sample of 0.5 mm thickness ($D = 0.5\ \mathrm{mm}^2 \cdot \mathrm{s}^{-1}$ and $\alpha = 3\ \mathrm{mm}^{-1}$). $S_{\mathrm{n,measured}}$ has been simulated by adding a 2 % random error to the calculated value of Eqs. 2 or 3. As can be seen, a clear minimum of g (the cross in Fig. 4) arises indicating that D and α are not degenerate and, therefore, they can be retrieved using the appropriate inversion algorithm.

2 Additional Effects

Now we study some additional effects that modify the photothermal signal recorded by the infrared detector and/or by the pyroelectric sensor.

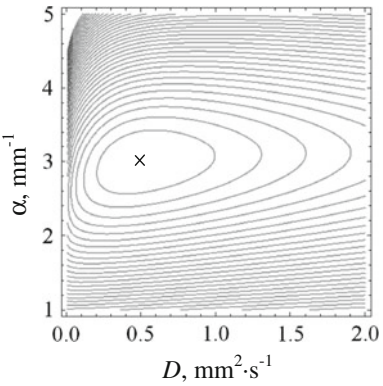

Fig. 4 Simulated contour plots of the residual function g for a semitransparent glass sample 0.5 mm thick ($D = 0.5\ \mathrm{mm}^2 \cdot \mathrm{s}^{-1}$ and $\alpha = 3\ \mathrm{mm}^{-1}$)

2.1 Multiple Reflections of the Light Beam

If the incident light crossing the semitransparent sample reaches the rear surface before vanishing, it will be reflected back and forth contributing to an increase in the sample temperature in PTR experiments and the average temperature of the pyroelectric sensor in PPE experiments. Numerical calculations indicate that the effect of the multiple reflections of the light beam is significant only for samples with $\alpha L < 2$ [15]. Anyway, it must be taken into account in order to retrieve accurate α and D values.

2.2 Transparency to Infrared Radiation

This effect only affects PTR measurements. Equation 2 is based on the assumption that the PTR signal is proportional to the sample surface temperature, i.e., the sample is opaque to IR wavelengths (in the case of HgCdTe detectors from 2 μm to 12 μm). This condition is fulfilled by metals and alloys, but not for most glasses and polymers. Actually, the visual appearance is not a reference to predict the infrared behavior. For instance, Ge is opaque to visible wavelengths, but completely transparent above 2 μm. As a consequence, it is necessary to evaluate the influence of the transparency to the infrared wavelengths on the measured voltage. If the sample is semitransparent to the infrared spectrum, the signal recorded by the infrared detector comes not only from its surface, but from the inner volume. If we define β as the effective infrared absorption coefficient for the sample (averaging the sample behavior from 2 μm to 12 μm), the signals recorded by the IR detector in the front and back configurations are [16]

$$S_{\mathrm{PTR,front/back}} \propto \int_{-L}^{0} \beta \mathrm{e}^{\beta z} T_{\mathrm{front/back}}(z)\, \mathrm{d}z, \tag{5}$$

where $T_{\mathrm{front}}(z)$ and $T_{\mathrm{back}}(z)$ are given by Eq. 1. The self-normalized PTR signal is given by

$$S_{\mathrm{PTR,n}} = \frac{S_{\mathrm{PTR,back}}}{S_{\mathrm{PTR,front}}}. \tag{6}$$

An analytical expression for $S_{\mathrm{PTR,n}}$ is obtained, which remains unchanged when exchanging the α and β values. This is the main limitation of the PTR technique to extract the thermal and optical parameters of solids. This issue can be overcome by performing several PTR measurements on the same sample, using heating lasers of different wavelengths for each measurement. This procedure would give different α values while the β value would remain constant.

Finally, note that the accurate retrieval of D and α using the PTR technique requires combining both effects: multiple reflections of the light beam and transparency to infrared radiation.

3 Experimental Results and Discussion

The experimental PTR setup is described in Ref. [15]. A solid-state laser beam ($\lambda = 532$ nm, 7 W), modulated by an acousto-optic modulator, was used to heat the sample. The beam was expanded to a diameter of 1 cm to guarantee 1-D heat propagation. Using plane mirrors, the laser was sent to the front or to the rear surface of the sample. The infrared radiation emitted from the sample was collected by an off-axis parabolic mirror system and detected by a HgCdTe sensor (2 μm to 12 μm). The voltage produced by the detector was amplified and then fed into a digital lock-in amplifier. A Ge window, which is opaque for visible wavelengths but transparent above 2 μm, is usually placed in front of the detector to prevent the green light of the laser from reaching the IR sensor. However, in this work a Ge-based spectral filter was used to reduce the transmission region of the detector (5 μm to 12 μm).

In the PPE setup the samples are placed on top of a $LiTaO_3$ pyroelectric crystal 0.5 mm thick. Indium tin oxide (ITO) electrodes are sputtered on both sides of the pyroelectric crystal. A very thin silicone grease layer, which is transparent to visible light, is used to assure the thermal contact. A diode laser ($\lambda = 656$ nm, 50 mW) has been used as the heating source. Its intensity is modulated by a periodic current managed by the computer and serving as the lock-in reference. Using a beam splitter, the laser beam is directed to the sample (back configuration) or to the pyroelectric crystal (front configuration). The PPE current produced by the detector has been fed into a digital lock-in amplifier.

In order to compare the ability of modulated PTR and PPE to characterize the thermal diffusivity and the optical absorption coefficient of solid slabs, we have performed measurements on a wide set of samples. First, we have measured opaque samples covering a wide range of diffusivities: rigid graphite, Ni, SiC (38 % porosity), vitreous carbon (Sigradur G), and carbon fiber reinforced (CFR) composite. In Table 1 we show the retrieved thermal diffusivities, which are in good agreement with the literature values.

We have also studied two optical filters of different optical absorption coefficients: a neutral density (ND) filter from Edmund Optics and a neutral density filter from Schott (NG 1). They are opaque to IR wavelengths above 5 μm. For each one we

Table 1 Comparison of the measurements of the thermal and optical properties of homogeneous samples using PTR and PPE techniques

Material	L (mm)	D ($mm^2 \cdot s^{-1}$) Literature	PTR measurements				PPE measurements		
			D ($mm^2 \cdot s^{-1}$)	α (mm^{-1}) $\lambda = 532$ nm	α (mm^{-1}) Cary Spectrometer	β (mm^{-1})	D ($mm^2 \cdot s^{-1}$)	α (mm^{-1}) $\lambda = 656$ nm	α (mm^{-1}) Cary Spectrometer
Graphite	2.57	87	89	–	∞	∞	85	–	∞
Ni	1.03	22	18	–	∞	∞	21	–	∞
Porous SiC	1.63	7	7.2	–	∞	∞	6.8	–	∞
Vitreous C	1.34	6	6	–	∞	∞	6	–	∞
CFR composite	0.85	0.5	0.51	–	∞	∞	0.51	–	∞
NDfilter	3.31	0.5–0.6	0.59	2.05	2.33	∞	0.54	1.99	1.96
NDfilter	2.12	0.5–0.6	0.57	2.1	2.33	∞	0.56	2.03	1.96
NDfilter	1.04	0.5–0.6	0.54	2.1	2.33	∞	0.55	1.9	1.96
Schott NG 1	0.478	0.5–0.6	0.48	10.5	11.1	∞	0.49	9.9	10.2
Schott NG 1	0.39	0.5–0.6	0.49	10.8	11.1	∞	0.48	9.8	10.2
Schott NG 1	0.27	0.5–0.6	0.51	10.7	11.1	∞	0.5	9.7	10.2
$LaMnO_3$	0.313	1.35	1.3	∞	∞	8.5	1.37	∞	∞
Cr_2O_3	0.761	3.8	3.6	∞	∞	6.7	3.8	∞	∞

Uncertainty in the retrieved values of D, α, and β is 5%

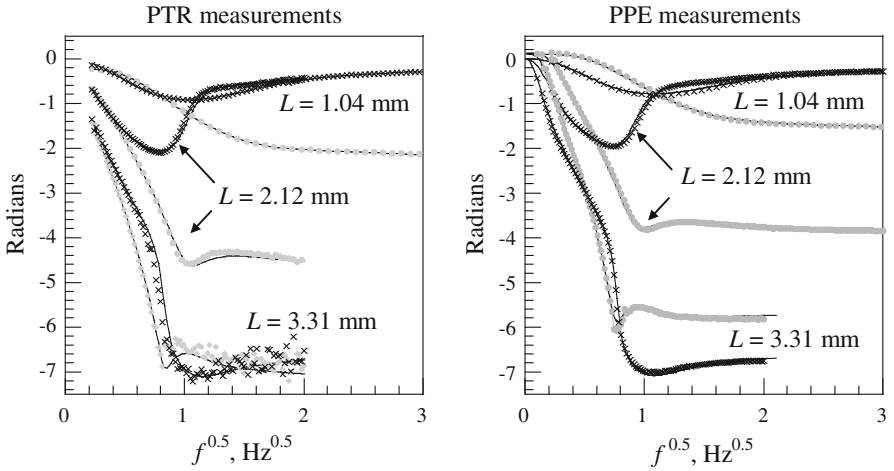

Fig. 5 Experimental values of $\ln(|S_n|)$ (*dots*) and $\Psi(S_n)$ (*crosses*) for three samples of the same neutral density filter (ND from Edmund Optics) but with different thicknesses. *Continuous lines* are the fits to Eqs. 2 or 3

have taken data on samples of different thicknesses in order to verify the self-consistency of the retrieved values. The experimental results for three different thicknesses of the ND filter are shown in Fig. 5. Dots correspond to the natural logarithm of the amplitude $\ln(|S_n|)$ and crosses for the phase $\Psi(S_n)$. The continuous lines are the fits to the model, including the multiple reflections of the light beam. As can be seen, PTR data are noisier than the PPE ones due to the smaller signal-to-noise ratio. This happens even though we use a 7 W laser for PTR measurements and a 50 mW laser for PPE measurements. The retrieved values of D and α are shown in Table 1. For each filter, the same D and α values are obtained within the experimental uncertainty (5 %) regardless of their thicknesses, confirming the reproducibility of the method. The retrieved α of each filter agrees with the value measured with a Cary spectrometer. The difference of α values obtained from PTR and PPE techniques is related to the different laser wavelengths used for the illumination (532 nm and 656 nm).

In addition, we have measured two metallic oxides, $LaMnO_3$ and Cr_2O_3, that are completely black, i.e., opaque to visible wavelengths, but semitransparent to IR wavelengths. Using the PPE setup, we have obtained parallel straight lines when representing $\ln(|S_{PPE,n}|)$ and $\Psi(S_{PPE,n})$ against $\sqrt{f}$. From their slopes we obtain the thermal diffusivity. However, PTR measurements show the influence of the transparency to IR wavelengths. By fitting the $\ln(|S_{PPE,n}|)$ and $\Psi(S_{PPE,n})$ data to the complete model we have retrieved D and β. Results are shown in Table 1. As can be seen, D values obtained from the two photothermal techniques are consistent within the experimental uncertainty.

Finally, we address the question of which (PTR or PPE) is the most appropriate technique to measure the thermo-optical properties of solid samples. The main advantage of the PPE technique is its high signal-to-noise ratio. In this way, power excitations of a few mW provide quasi-noise free signals while power excitations of the order

Table 2 Comparison of the advantages (capital letters) and limitations (lower-case letters) between PTR and PPE techniques

PTR	PPE
Low signal-to-noise ratio	HIGH SIGNAL-TO-NOISE RATIO
Laser intensity ($W \cdot m^{-2}$)	LASER INTENSITY ($mW \cdot m^{-2}$)
BIG SAMPLES	Small samples (<1 cm^2)
NON-CONTACT TECHNIQUE	Contact technique
Extended light beam	EXTENDED OR FOCUSED LIGHT BEAM
Influence of IR transparency	INSENSITIVE TO IR TRANSPARENCY

of watts are needed in PTR measurements. Low power excitation means small thermal gradients inside the sample and therefore PPE is specially suited to characterize the thermal properties of phase transitions. On the other hand, the transparency of the sample to IR radiation complicates the analysis of the PTR signal. The main drawback of the PPE method is that it is a contact technique valid for small samples (<1 cm^2), while PTR is a contactless technique allowing in situ measurements of big samples in industrial environments. Another interesting question is that large spots have to be used in PTR measurements in order to guarantee 1-D heat propagation. On the contrary, PPE measurements are independent of the light spot size since the pyroelectric voltage is proportional to the average temperature of the sensor [17]. In Table 2 we summarize the advantages and limitations of both photothermal techniques. We can conclude that both techniques are complementary and should be used alternatively depending on the characteristics of the sample to be measured.

Acknowledgments This work has been supported by the Ministerio de Educación y Ciencia (MAT2008-01454), by the Ministerio de Ciencia e Innovación (MAT2011-23811), by Gobierno Vasco (IT351-10) and by UPV/EHU (UFI11/55).

References

1. P.E. Nordal, S.O. Kanstad, Phys. Scr. **20**, 659 (1979)
2. H. Coufal, Appl. Phys. Lett. **45**, 516 (1984)
3. A. Mandelis, Chem. Phys. Lett. **108**, 388 (1984)
4. M. Chirtoc, in *Thermal Wave Physics and Related Photothermal Tecniques: Basic Principles and Recent Developments*, ed. by E. Marín (Transworld Research Network, Trivandrum, 2009), pp. 29–63
5. M. Chirtoc, D. Dadarlat, D. Bicanic, J.S. Antoniow, M. Egée, in *Progress in Photothermal and Photoacoustic Science and Technology*, vol. 3, ed. by A. Mandelis, P. Hess (SPIE, Bellingham, Washington, 1997), pp. 185–251
6. U. Zammit, M. Marinelli, F. Mercuri, S. Paoloni, F. Scuderi, Rev. Sci. Instrum. **82**, 121101 (2011)
7. G.C. Wetsel, F.A. McDonald, Appl. Phys. Lett. **30**, 252 (1977)
8. Y.C. Teng, B.S.H. Royce, J. Opt. Soc. Am. **70**, 557 (1980)
9. A. Mandelis, J. Appl. Phys. **54**, 3404 (1983)
10. J.A. Balderas-López, A. Mandelis, Rev. Sci. Instrum. **74**, 5219 (2003)
11. A. Rosencwaig, A. Gersho, J. Appl. Phys. **47**, 64 (1976)
12. S.O. Kanstad, P.E. Nordal, Can. J. Phys. **64**, 1155 (1986)
13. M. Chirtoc, G. Mihailescu, Phys. Rev. B **40**, 9606 (1989)
14. S. Delenclos, M. Chirtoc, A.H. Sahraoui, C. Kolinski, J.M. Buisine, Rev. Sci. Instrum. **73**, 2773 (2002)

15. R. Fuente, E. Apiñaniz, A. Mendioroz, A. Salazar, J. Appl. Phys. **110**, 033515 (2011)
16. H.G. Walther, U. Seidel, W. Karpen, G. Busse, Rev. Sci. Instrum. **63**, 5479 (1992)
17. M. Rombouts, L. Froyen, A.V. Gusarov, E.H. Bentefour, C. Glorieux, J. Appl. Phys. **97**, 024905 (2005)